






ORIGINAL ARTICLE

Multimerin 1 supports platelet function in vivo and binds to specific GPAGPOGPX motifs in fibrillar collagens that enhance platelet adhesion

Alexander Leatherdale¹ | D'Andra Parker¹ | Subia Tasneem¹ | Yiming Wang^{2,3} | Dominique Bihan⁴ | Arkadiusz Bonna⁴ | Samir W. Hamaia⁴ | Peter L. Gross⁵  | Heyu Ni^{2,3}  | Bradley W. Doble⁶  | David Lillicrap⁷ | Richard W. Farndale⁴ | Catherine P. M. Hayward^{1,8}  

¹Pathology and Molecular Medicine, McMaster University, Hamilton, ON, Canada

²Laboratory Medicine and Pathobiology, Keenan Research Centre, Li Ka-Shing Knowledge Institute, St. Michael's Hospital, University of Toronto, Toronto, ON, Canada

³Canadian Blood Services Centre for Innovation, Ottawa, ON, Canada

⁴Biochemistry, Downing Site, University of Cambridge, Cambridge, UK

⁵Medicine, Thrombosis and Atherosclerosis Research Institute, McMaster University, Hamilton, ON, Canada

⁶Biochemistry and Biomedical Sciences, McMaster Stem Cell and Cancer Research Institute, McMaster University, Hamilton, ON, Canada

⁷Pathology and Molecular Medicine, Richardson Laboratory, Queen's University, Kingston, ON, Canada

⁸Hamilton Regional Laboratory Medicine Program, and Department of Medicine, McMaster University, Hamilton, ON, Canada

Correspondence

Catherine P. M. Hayward, Department of Pathology and Molecular Medicine, McMaster University, 1200 Main St West, HSC 2N29A, Hamilton, ON L8N 3Z5, Canada.
Email: haywrdc@mcmaster.ca

Present address

Arkadiusz Bonna and Richard W. Farndale, CambCol Laboratories Ltd, Ely, UK

Funding information

Canadian Institutes of Health Research, Grant/Award Number: 119540, FDN-154285 and MOP 133474; British Heart Foundation, Grant/Award Number: RG/15/4/31268; Wellcome Trust, Grant/Award Number: 094470/Z/10/Z; Heart and Stroke Foundation of Canada, Grant/Award Number: NA7214 and T6586

Abstract

Background: Multimerin 1 (human: MMRN1, mouse: Mmnr1) is a homopolymeric, adhesive, platelet and endothelial protein that binds to von Willebrand factor and enhances platelet adhesion to fibrillar collagen ex vivo.

Objectives: To examine the impact of Mmnr1 deficiency on platelet adhesive function, and the molecular motifs in fibrillar collagen that bind MMRN1 to enhance platelet adhesion.

Methods: Mmnr1-deficient mice were generated and assessed for altered platelet adhesive function. Collagen Toolkit peptides, and other triple-helical collagen peptides, were used to identify multimerin 1 binding motifs and their contribution to platelet adhesion.

Results: MMRN1 bound to conserved GPAGPOGPX sequences in collagens I, II, and III (including GPAGPOGPI, GPAGPOGPV, and GPAGPOGPQ) that enhanced activated human platelet adhesion to collagen synergistically with other triple-helical

Manuscript handled by: X. Long Zheng

Final decision: X. Long Zheng, 06 November 2020

Alexander Leatherdale, D'Andra Parker, and Subia Tasneem contributed equally to this study, which was presented in abstract form at the 59th annual meeting of the American Society of Hematology, Atlanta, GA, 11 December 2017.

This is an open access article under the terms of the Creative Commons Attribution License, which permits use, distribution and reproduction in any medium, provided the original work is properly cited.

© 2020 The Authors. *Journal of Thrombosis and Haemostasis* published by Wiley Periodicals LLC on behalf of International Society on Thrombosis and Haemostasis

collagen peptides ($P < .05$). *Mmrn1*^{-/-} and *Mmrn1*^{+/-} mice were viable and fertile, with complete and partial platelet *Mmrn1* deficiency, respectively. Relative to wild-type mice, *Mmrn1*^{-/-} and *Mmrn1*^{+/-} mice did not have overt bleeding, increased median bleeding times, or increased wound blood loss ($P \geq .07$); however, they both showed significantly impaired platelet adhesion and thrombus formation in the ferric chloride injury model ($P \leq .0003$). *Mmrn1*^{-/-} platelets had impaired adhesion to GPAGPOGPX peptides and fibrillar collagen ($P \leq .03$) and formed smaller aggregates than wild-type platelets when captured onto collagen, triple-helical collagen mimetic peptides, von Willebrand factor, or fibrinogen ($P \leq .008$), despite preserved, low shear, and high shear aggregation responses.

Conclusions: Multimerin 1 supports platelet adhesion and thrombus formation and binds to highly conserved, GPAGPOGPX motifs in fibrillar collagens that synergistically enhance platelet adhesion.

KEYWORDS

blood platelets, fibrillar collagens, multimerin, platelet adhesiveness, von Willebrand factor

1 | INTRODUCTION

Platelet adhesion is a critical step in hemostasis and thrombosis that allows platelets to localize and accumulate at sites of vessel injury or thrombus formation. Multimerin 1 (human: MMRN1, mouse: *Mmrn1*) is a large, soluble, homopolymeric adhesive glycoprotein that is synthesized and stored by megakaryocytes/platelets and endothelial cells for regulated release, but is undetectable in normal plasma.¹⁻⁴ When released, MMRN1 supports platelet adhesion through shear-dependent mechanisms involving activated $\alpha_{IIb}\beta_3$ and $\alpha_v\beta_3$ under static conditions and low shear flow conditions ($\leq 150 \text{ s}^{-1}$), and involving von Willebrand factor (human: VWF; mouse: *Vwf*) and GPIIb α , but not β_3 integrins, under high shear flow (1500 s^{-1}).^{5,6} MMRN1 binds to VWF with high affinity through a two-site, two-step interaction with the VWF A1 and A3 domains that enhances platelet adhesion to immobilized VWF at high shear flow.⁷ MMRN1 also enhances platelet adhesion to vascular fibrillar collagens I and III and Horm collagen (equine collagen I, ~95%, and III, ~5%) under high shear flow through mechanisms requiring VWF and GPIIb α ⁶ and uncharacterized motifs in collagen that support MMRN1 binding. The impact of *Mmrn1* deficiency on platelet function has not been fully characterized.

Similar to MMRN1, the adhesive proteins VWF, fibronectin (FN), vitronectin (VN), and fibrin self-associate to form large homopolymers,⁸⁻¹⁴ and bind to $\alpha_{IIb}\beta_3$ on platelets¹⁵⁻²⁰ to mediate aggregate formation. Additionally, thrombospondin-1 (TSP-1) helps to cross-link platelets by self-associating and binding $\alpha_{IIb}\beta_3$ -bound fibrinogen (FG).²¹ These interactions create large macromolecular complexes that increase the likelihood of platelet-platelet collisions and the avidity of platelet-matrix or platelet-platelet interactions.²² We postulated that the large MMRN1 homopolymers released by platelets and endothelial cells might similarly enhance platelet-matrix or platelet-platelet interactions, as *Mmrn1*^{-/-}*Snca*^{-/-} mice (evaluated by the ferric chloride [FeCl₃] mesenteric vessel injury model) have impaired platelet

Essentials

- Multimerin 1 (*Mmrn1*) is a homopolymeric protein that supports platelet adhesion in vitro.
- *Mmrn1*-deficient mice and collagen peptides were used to assess *Mmrn1* contributions to platelet function.
- *Mmrn1* loss impaired platelet adhesion in vivo and to GPAGPOGPX motifs in collagens in vitro.
- *Mmrn1* contributes to platelet function and binds to adhesive GPAGPOGPX motifs in collagen.

adhesion and thrombus formation in vivo, and impaired platelet adhesion to collagen in vitro, that are corrected by exogenous MMRN1.²³

We generated *Mmrn1*-deficient (*Mmrn1*^{-/-}) mice to: (a) determine the impact of selective *Mmrn1* loss on platelet adhesion and thrombus formation in vivo; (b) identify additional adhesive ligands for MMRN1/*Mmrn1*, and the impact of *Mmrn1* deficiency on platelet adhesion and aggregation; and (c) investigate the motifs in collagen that support binding to MMRN1. We demonstrate that *Mmrn1* contributes to platelet adhesion and thrombus formation in vivo and update the current model of platelet adhesion to collagen to include GPAGPOGPX, a conserved MMRN1/*Mmrn1* binding motif that synergistically enhances platelet adhesion.

2 | METHODS

The study was conducted in accordance with the recently revised Declaration of Helsinki with approval of the Hamilton Integrated Research Ethics Board, McMaster University Animal Research Ethics Board, and St. Michael's Animal Care Committee.

Mmrn1-deficient mice were generated as outlined in Appendix S1 in supporting information. Experiments were done with wild-type, *Mmrn1*^{-/-}, and *Mmrn1*^{+/-} mice obtained from crosses of *Mmrn1*^{+/-} mice that were regenerated every three to five generations by additional crosses, as outlined in Appendix S1.

2.1 | Evaluation of mouse bleeding after tail transection

Bleeding times (BT) and blood loss following tail transection 1.5 mm from the distal tip were evaluated as described.²⁴ BT were recorded as 900 seconds if bleeding had not stopped by then.

2.2 | Blood collection

Murine blood was obtained by terminal exsanguination of anesthetized mice after carotid artery cannulation.²⁵ Human blood was collected from general population controls with written informed consent.

2.3 | Mouse blood counts and glycoprotein analysis

Complete blood counts were determined using a Hemavet 950 instrument (Drew Scientific Inc). Platelet *Mmrn1* content was evaluated by western blot analysis of platelet lysate after reduced sodium dodecyl sulfate polyacrylamide gel electrophoresis (SDS-PAGE) using polyclonal rabbit antibodies (SC-367225, Santa Cruz Biotechnology, Inc).²⁶ Plasma and platelet Vwf were quantified by enzyme-linked immunosorbent assay (ELISA) using polyclonal rabbit anti-human VWF (A0082 and P0226, DAKO Canada Inc) and pooled normal mouse plasma (NMP) as the standard (results reported as % NMP) as described.^{27,28} Flow cytometry was performed as described,²⁵ using: fluorescein isothiocyanate (FITC)-labeled rat anti-mouse Gplb α (CD42b; clone Xia.G5), anti-mouse/rat P-selectin (CD62P; Emfret Analytics; clone Wug.E9) and rat anti-mouse β_1 (CD29; BD Biosciences; clone Ha2/5), and phycoerythrin (PE)-labeled hamster anti-mouse β_3 (CD61, BD Biosciences; clone 2C9.G2) and rat anti-mouse activated $\alpha_{IIb}\beta_3$ (CD41/CD61, Emfret Analytics; clone JON/A).

2.4 | Intravital microscopy

Platelet adhesion and thrombus formation in mesenteric arterioles treated with 250 mmol/L FeCl₃ were evaluated as described,²³ to assess: (a) fluorescent platelet deposition on the vessel wall per minute, between 3 and 5 minutes following injury, (b) time to form the first 20 μ m diameter thrombus, and (c) vessel occlusion time.

2.5 | Preparation of recombinant human multimerin 1

Recombinant (r) human MMRN1 was affinity purified from media of stably transfected human embryonic kidney (HEK)-293 cells and assessed for concentration and purity by ELISA, western blotting, and silver staining as described.^{4,5}

2.6 | Protein binding assays

rMMRN1 binding to immobilized human FG (\pm pre-treatment with 0.2 U/mL thrombin to induce fibrin formation), FN, or triple-helical collagen peptides was evaluated based on methods described,⁶ using Immulon 2 HB flat-bottom plates (Thermo Fisher Scientific) coated (overnight, 4°C) with 1 μ g/well protein or peptide.

2.7 | Assays of platelet adhesion under shear

Endpoint and real-time analyses of mouse platelet adhesion were evaluated as described,⁷ except Vena8Fluoro+ (Cellix Ltd) biochips were coated (overnight, 4°C) with: 100 μ g/mL Horm collagen (Nycomed Austria GmbH), 10 U/mL recombinant (r)Vwf, 100 μ g/mL murine fibrinogen (Fg; \pm 15 minutes pre-treatment with 0.2 U/mL thrombin after immobilization to convert to fibrin, as described)⁵ (Molecular Innovations), 100 μ g/mL murine fibronectin (Fn; Molecular Innovations), or combinations of triple-helical collagen peptides (50 μ g/mL of each, or 100 μ g/mL GPP). For testing adhesion of *Mmrn1*^{-/-} and wild-type platelets in whole blood to Fg, fibrin, Fn, and rVwf, blood was collected into 93 μ mol/L (50 μ g/mL) PPACK, or into 93 μ mol/L PPACK with 2 U/mL heparin for experiments with Horm collagen,^{6,23} before labeling platelets with 4 μ mol/L DiOC6(3) (Enzo Life Sciences; 10 minutes, 37°C, $\geq 5 \times 10^8$ platelets/mL). *Mmrn1*^{-/-} and wild-type whole blood for real-time perfusion assays was collected into 10 U/mL heparin.²³ For assays with washed mouse platelets, samples were prepared and labeled with 4 μ mol/L DiOC6(3) as described⁷ and incubated with 10 μ g/mL crosslinked collagen-related peptide (CRP-XL; sequence: GCO[GPO₁₀]GCOG, hereafter referred to as CRP) to induce *Mmrn1* release before testing.

2.8 | Mouse platelet aggregation

Light transmission aggregometry (LTA) and whole blood aggregometry (WBA) were performed using: *Mmrn1*^{-/-} and wild-type mouse samples; a Chrono-Log aggregometer (Havertown, PA; settings as recommended by the manufacturer)²³; mouse whole blood, platelet-rich plasma (PRP), and gel-filtered platelets (GFP, thrombin-induced aggregation only), with PRP and GFP adjustment to

2.5×10^8 platelets/mL; and the agonists 5 $\mu\text{g/mL}$ Horm collagen (Helena Laboratories), 10–20 $\mu\text{mol/L}$ adenosine diphosphate (ADP; Sigma Aldrich Canada), 500 $\mu\text{mol/L}$ murine thrombin receptor-activating peptide (TRAP; AYPGKF-NH₂), and 0.5–1.0 U/mL human thrombin (GFP only).

Shear-induced platelet aggregation (SIPA) was evaluated using a HAAKE Mars rheometer (Thermo Electron Corporation) fitted with a C35/0.5° Ti (35 mm diameter) cone. Shear stress τ and shear rate γ were calculated automatically by HAAKE RheoWin 3 software. Whole blood from *Mmrn1*^{-/-} and wild-type mice was collected in 1:10 (v/v) 3.2% sodium citrate, and supplemented with 5 mmol/L CaCl₂ and 93 $\mu\text{mol/L}$ PPACK (to promote aggregation and prevent clotting, respectively) immediately before loading samples. Blood was sheared by the rotating cone in a 0.3 mm gap for 1 minute at room temperature before fixation with 1:4 (v/v) 0.625% paraformaldehyde (0.5% final). Fixed platelets were labelled in the dark using 1:8.3 (v/v) of anti-mouse GpIb α (CD42b, Emfret Analytics) for 15 minutes before diluting samples 1:200 (v/v) in phosphate buffered saline and adding BD™ Liquid Counting Beads (165 beads/mL, Becton, Dickinson and Company, BD Biosciences). After mixing by gentle pipetting, 50 000 events were collected with a Beckman Coulter® Epics® XL-MCL™ flow cytometer and Expo32™ software (Beckman Coulter). Events were gated for single platelets (defined by forward and side scatter characteristics) using FlowJo™ 10 (Becton, Dickinson and Company). Platelet concentration was estimated by comparing platelet and counting bead events to determine the % reduction in platelet concentration for sheared relative to unsheared samples.

2.9 | Peptide synthesis

Triple-helical Collagen Toolkit II and III peptides (full sequences reported elsewhere) and derivatives (sequences in Table S1 in supporting information) were generated as described,²⁹ along with: CRP (GPVI ligand to activate platelets),^{30,31} GFOGER (high-affinity ligand for platelet integrin $\alpha_2\beta_1$),³² Toolkit peptide III-23 (containing the VWF ligand GPRGQOGVMGFO),³³ and GPP (negative control).

2.10 | Static platelet adhesion assays

Static platelet adhesion was evaluated largely as described,³⁴ using *Mmrn1*^{-/-} and wild-type samples and wells pre-coated with: 1 $\mu\text{g/well}$ rMMRN1, murine Fg (\pm pre-treatment with 0.2 U/mL thrombin), murine Fn, Horm collagen or collagen peptides (0.5 $\mu\text{g/well}$ of each of two peptides or 0.33 $\mu\text{g/well}$ of each of three peptides), or a range of peptide concentrations for titrations, before blocking and adding washed platelets (prepared as described,³⁴ final: human: 1.6×10^8 platelets/mL, 8×10^6 platelets/well; mouse: 1.8×10^8 platelets/mL, 9×10^6 platelets/well). Unless otherwise specified, platelets were pre-treated (without stirring) with 10 $\mu\text{g/mL}$ of CRP (5 minutes, 37°C) immediately before testing.

2.11 | Quantification of platelet adhesion and sizes of adherent platelet aggregates

Percent surface area covered by platelets was estimated using ImageJ (National Institutes of Health), and sizes of captured platelet aggregates on surfaces were estimated using representative regions (in-focus) at the center of microcapillary channels, using the following objectives and areas: Horm collagen: 40 \times objective, $\sim 60 \text{ mm}^2$ square, 1020 \times 1020 pixels; rVwf, fibrin(ogen), fibronectin, and collagen peptides: 20 \times objective, $\sim 20 \text{ mm}^2$ squares, 515 \times 515 pixels. Grayscale images were converted to binary using the Threshold tool before separating features using the Watershed tool and counting using the Analyze Particles tool. As platelet aggregate sizes on Horm collagen varied greatly (~ 1 – $40\,000 \mu\text{m}^2$), data were binned and evaluated by frequency plots. Platelet aggregates captured onto rVwf, fibrin(ogen), fibronectin, and collagen peptides (sizes: ~ 1 – $5000 \mu\text{m}^2$) were evaluated using mean feature sizes/image.

2.12 | Statistical analyses

Two-tailed independent or paired Student's *t*-tests were used to evaluate data with normal distributions. Mann-Whitney *U*-tests were used to evaluate data with non-normal distributions. One-way or repeated measures analysis of variance were used to evaluate data with more than two groups ($\alpha < 0.05$ considered significant). Bonferroni correction was used for post hoc multiple comparisons where $k \leq 6$ or the Holm-Sidak method where $k > 6$, with $\alpha < 0.05$ considered significant for each family of comparisons. One-tailed *z* test of population proportions was used to evaluate proportional data. Unless stated otherwise, data are reported as mean \pm standard error of the mean (SEM).

3 | RESULTS

3.1 | Mice homozygous for *Mmrn1* E3 deletion are viable and fertile, with normal platelet aggregation responses and a minor prolongation of bleeding time

Mice homozygous for the E3-deleted *Mmrn1* allele (*Mmrn1*^{-/-}; Figure 1A) were viable and fertile, and lacked detectable platelet *Mmrn1* (Figure 1B), whereas *Mmrn1*^{+/-} mice had reduced platelet *Mmrn1* relative to wild-type mice (Figure 1B). *Mmrn1*^{-/-} and *Mmrn1*^{+/-} mice had normal blood counts and Vwf levels (Table S2 in supporting information) and no overt bleeding or other phenotypic abnormalities. Additionally, compared to wild-type platelets, *Mmrn1*^{-/-} and *Mmrn1*^{+/-} platelets showed comparable resting surface expression of glycoprotein (Gp)Ib α (CD42b) and β_1 (CD29) and β_3 integrins (CD61; Figure 1C), comparable thrombin-induced platelet P-selectin expression (CD62P; Figure S1A in supporting information) and only minor differences in activated $\alpha_{IIb}\beta_3$ expression ($P < .01$; Figure S1B). BT (Figure 1D), the proportion of mice

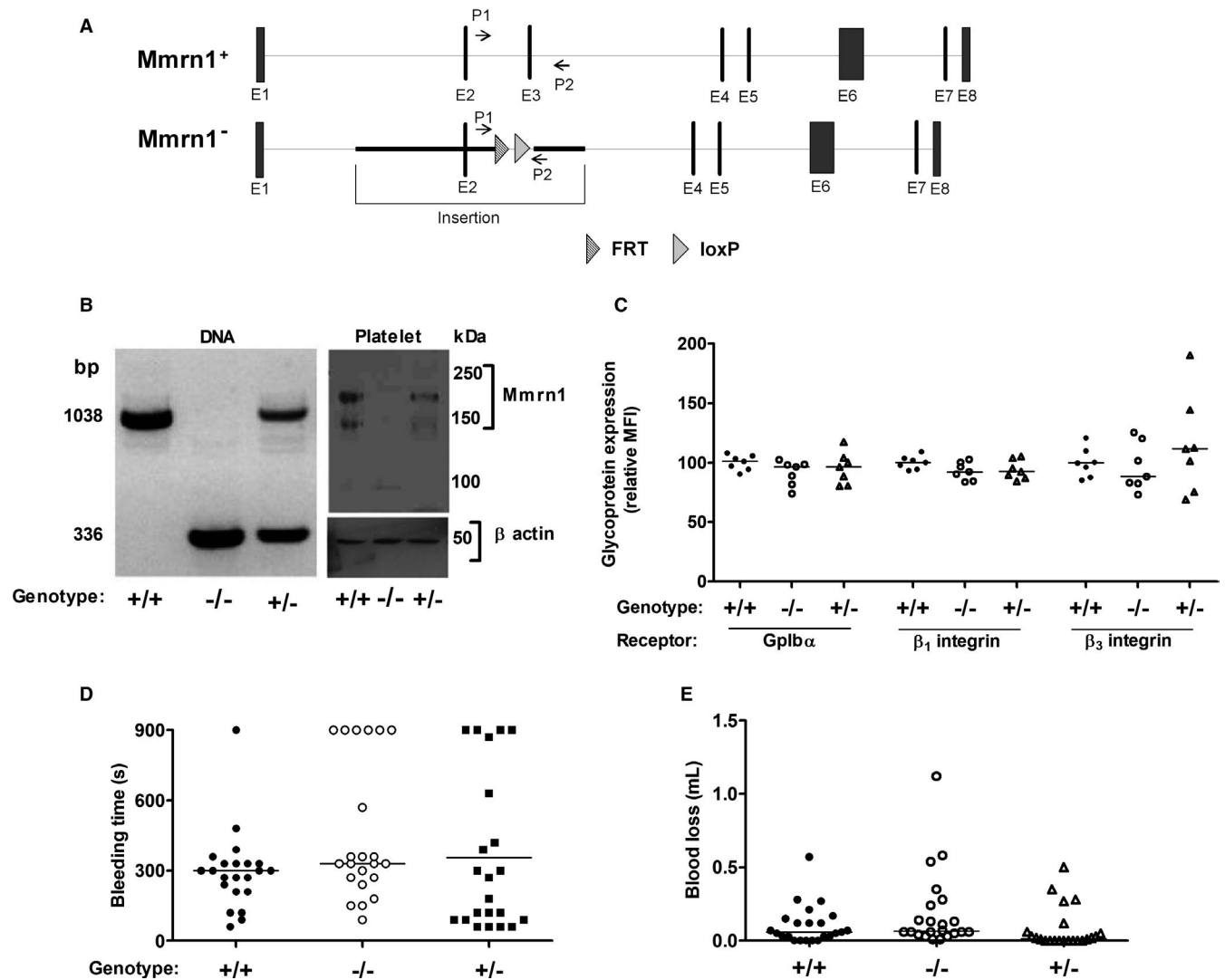


FIGURE 1 Evaluation of genotype, platelet phenotype, bleeding time, and wound blood loss of mice homozygous for multimerin 1 (*Mmrrn1*) E3 deletion. **A**, Comparison of the *Mmrrn1* gene in wild-type (top) and *Mmrrn1*-deficient mice lacking E3 (bottom) with binding sites for primers P1 and P2 used for *Mmrrn1* genotyping. The darker line indicates the region of *Mmrrn1* replaced by the targeting vector via homologous recombination. **B**, Genotype (left) and phenotype (right) of *Mmrrn1*^{+/+}, *Mmrrn1*^{+/-}, and *Mmrrn1*^{-/-} mice analyzed by polymerase chain reaction and western blotting of platelet lysate using rabbit anti-MMRN1, respectively. **C**, Flow cytometry quantification of platelet membrane Gplbα, β₁ integrin, and β₃ integrin (n = 7 per genotype). **D**, Bleeding time and **E**) wound blood loss following distal tip tail transection (at a diameter of 1.5 mm), measured up to 900 s (n = 22 mice/group). Panels C–E compare data for *Mmrrn1*^{+/+} (solid circles), *Mmrrn1*^{+/-} (open triangles), and *Mmrrn1*^{-/-} (open circles) mice

that did not stop bleeding by 900 seconds (6/22 versus 6/22 versus 1/22; $P \geq .09$) and BT wound blood loss (Figure 1E) were not significantly different for wild-type, *Mmrrn1*^{+/-}, and *Mmrrn1*^{-/-} mice even when the comparisons were extended to 22 mice per group ($P \geq .07$).

Platelets from *Mmrrn1*^{-/-} mice showed: normal low shear LTA responses to 0.5–1.0 U/mL thrombin ($P \geq .37$; Figure S2A,B in supporting information), TRAP, collagen, and 10–20 μmol/L ADP ($P \geq .13$; Figure S2C–F); normal WBA responses to collagen ($P \geq .49$, Figure S3); and normal SIPA over a range of shear rates (5000–15 000 s⁻¹; $P \geq .49$, Figure S4).

3.2 | *Mmrrn1* loss impairs platelet adhesion, thrombus formation, and vessel occlusion in vivo

In the FeCl₃-induced mesenteric vessel injury model, both *Mmrrn1*^{-/-} and *Mmrrn1*^{+/-} mice showed impaired platelet localization between 3 and 5 minutes following injury ($P < .001$; Figure 2A,B), and delayed appearance of the first large thrombus (≥ 20 μm; $P < .001$; Figure 2C), compared to wild-type mice, with 2/9 *Mmrrn1*^{-/-}, 3/7 *Mmrrn1*^{+/-} versus 0/9 *Mmrrn1*^{+/+} mice failing to form a thrombus ≥ 20 μm ($P \geq .067$; Videos S1–S3 [in supporting information], respectively, show representative data for these mice).

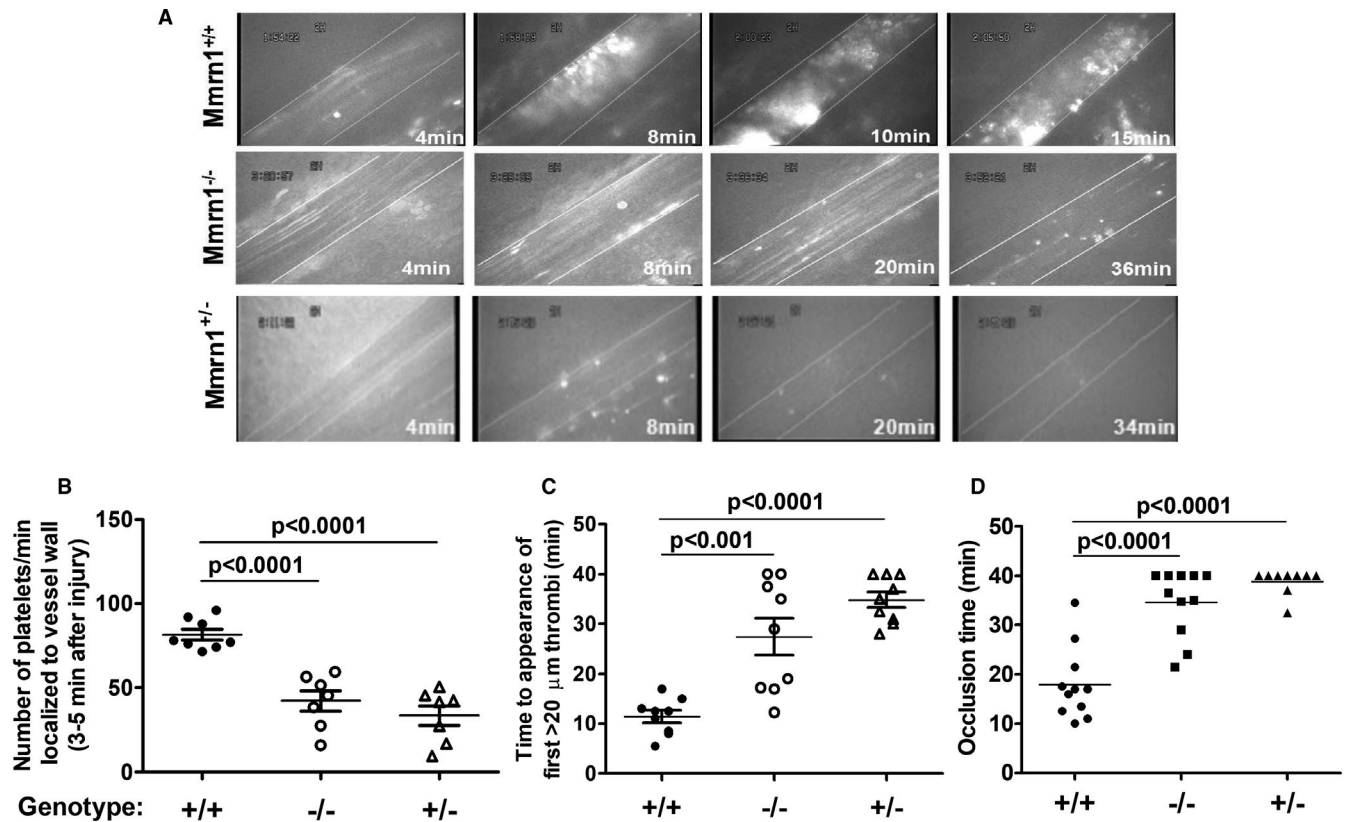


FIGURE 2 Thrombus formation in ferric chloride-injured mesenteric vessels of mice with and without multimerin 1 (*Mmrn1*) E3 deletion. A, Representative images show calcein acetoxyethyl (AM) ester-labeled platelet deposition and thrombus formation, captured using a Zeiss Axiovert 135 inverted epifluorescence microscope (Zeiss Oberkochen) and recorded on videotape (original magnification $\times 32$; see representative Videos S1-S3 in supporting information) at different time points after ferric chloride injury, as indicated. B, Number of platelets localized to the vessel wall 3 to 5 minutes following exposure to ferric chloride (number of mice assessed/genotype: *Mmrn1*^{+/+}: n = 8; others: n = 7). C, Time until the appearance of the first platelet-rich thrombus $\geq 20 \mu\text{m}$ in mice (n = 9 mice assessed/genotype). D, Time until total vessel occlusion (measured up to 40 minutes; number of mice assessed/genotype: *Mmrn1*^{+/+}: n = 9; others: n = 11) mice. Symbols (panels B-D) indicate *Mmrn1*^{+/+} (solid circle), *Mmrn1*^{-/-} (open circle), and *Mmrn1*^{+/-} (open triangle) mice

When large thrombi formed in arterioles of *Mmrn1*^{-/-} or *Mmrn1*^{+/-} mice, small platelet aggregates readily dissociated without re-associating downstream. Although 11/11 *Mmrn1*^{+/+} mice formed an occlusive thrombus by 10 to 35 minutes after FeCl_3 -induced injury, 3/8 *Mmrn1*^{-/-} mice and 7/7 *Mmrn1*^{+/-} mice failed to form an occlusive thrombus by 40 minutes ($P \leq .014$ for comparisons with *Mmrn1*^{+/+} mice; $P \geq .29$ for *Mmrn1*^{-/-} to *Mmrn1*^{+/-} mice comparisons; Figure 2D).

3.3 | *Mmrn1* loss selectively impairs platelet adhesion

In high shear flow experiments (1500 s^{-1}), with whole blood, both *Mmrn1*^{-/-} and *Mmrn1*^{+/-} platelets showed reduced adhesion to Horm collagen and failed to form the large adherent aggregates seen with wild-type platelets ($P \leq .008$, Figure 3A). Real-time analyses of the findings for *Mmrn1*^{-/-} and *Mmrn1*^{+/-} samples (Videos S4 and S5 in supporting information, respectively), indicated that *Mmrn1* deficiency was associated with less initial adhesion to collagen, and slower growth of platelet aggregates on collagen.

Static platelet adhesion experiments verified that *Mmrn1* deficiency impaired platelet adhesion to Horm collagen ($P = .03$; Figure 3B), without altering platelet adhesion to the triple-helical collagen peptide GFOGER that functions as a high-affinity $\alpha_2\beta_1$ ligand ($P = .49$; Figure 3C). *Mmrn1* deficiency also impaired platelet adhesion to Horm collagen in low shear flow (300 s^{-1}) conditions (Figure S5 in supporting information).

In high shear flow adhesion experiments (1500 s^{-1}), *Mmrn1*^{-/-} and *Mmrn1*^{+/-} platelets showed similar adhesion to rVwf using whole blood ($P = .13$; Figure 4A) and washed platelets ($P = .7$; Figure S6 in supporting information), although *Mmrn1*^{-/-} platelets were captured into smaller aggregates under these conditions ($P < .0001$).

Although rMMRN1 showed binding to human FG, fibrin, and FN (Figure S7A in supporting information; capitalized abbreviations indicate human proteins and mixed-case abbreviations indicate mouse proteins), activated *Mmrn1*^{-/-} and *Mmrn1*^{+/-} platelets showed comparable static adhesion to these proteins ($P \geq .14$, Figure S7B). The $\alpha_{\text{IIb}}\beta_3$ blocking antibody 9D2 similarly reduced the adhesion of activated *Mmrn1*^{-/-} and *Mmrn1*^{+/-} platelets to rMMRN1 and other $\alpha_{\text{IIb}}\beta_3$ ligands (Figure S7C). In low shear flow (300 s^{-1}) adhesion assays with

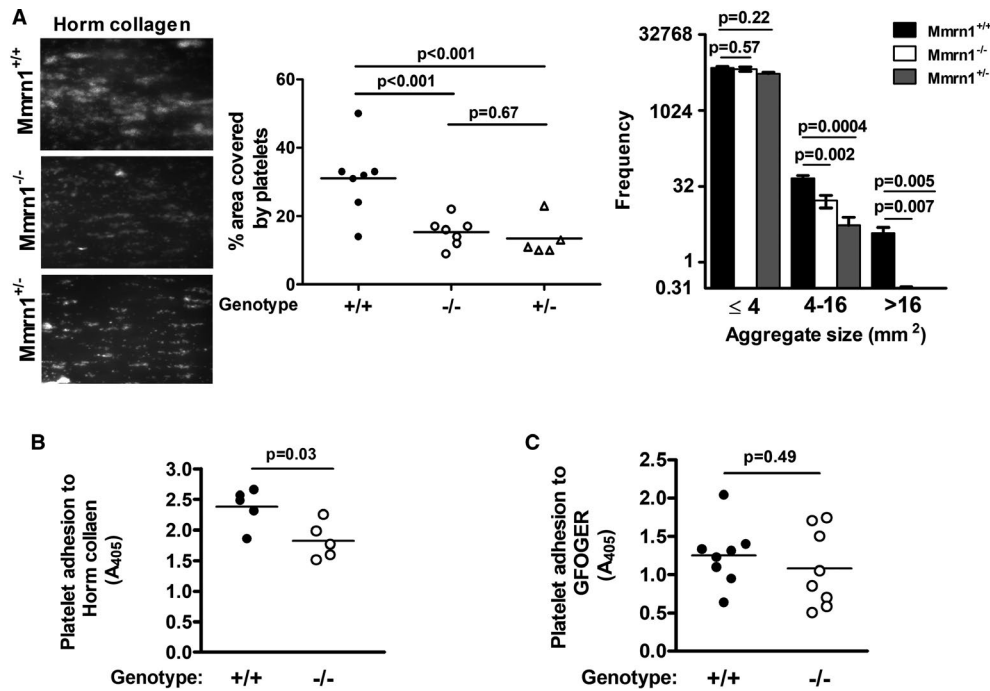


FIGURE 3 Effect of multimerin 1 (*Mmrn1*) deficiency on platelet adhesion to Horm collagen and GFOGER. A, Comparison of *Mmrn1*^{-/-}, *Mmrn1*^{+/-}, and wild-type platelet adhesion to Horm collagen, tested at high shear (1500 s^{-1}), assessed using representative images DiOC6(3)-labeled platelets (left) and quantitative analyses of the surface area covered by platelets (middle) and the average frequency of different-sized platelet aggregates captured onto collagen (right) (number of mice/genotype: *Mmrn1*^{+/-}: $n = 4$, others: $n = 6$). Panels (B) and (C) show static adhesion of collagen-related peptide-activated platelets tested with: (B) Horm collagen ($n = 5$ mice/group) and (C) GFOGER ($n = 8$ mice/group; *Mmrn1*^{+/-} mice not tested). Symbols indicate data for *Mmrn1*^{+/+} (solid), *Mmrn1*^{+/-} (open triangle), and *Mmrn1*^{-/-} (open circle) mice

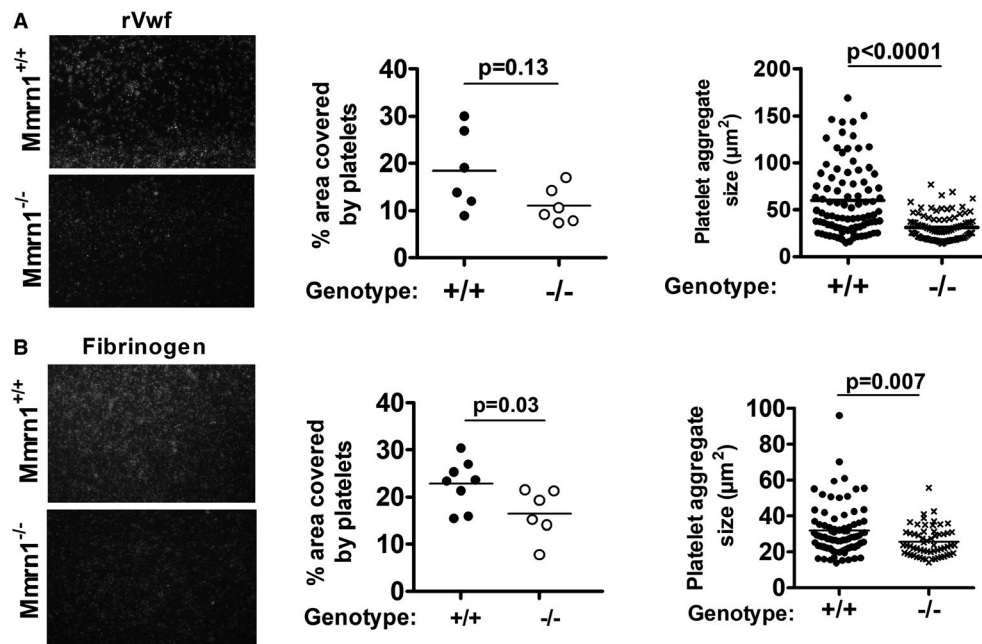


FIGURE 4 The effect of multimerin 1 (*Mmrn1*) deficiency on high shear (1500 s^{-1}) platelet adhesion to recombinant Vwf and low shear (300 s^{-1}) platelet adhesion to immobilized murine fibrinogen. Adhesion of wild-type and *Mmrn1*^{-/-} platelets was tested using whole blood and evaluated by representative images of adherent DiOC6(3)-labeled platelets (left; captured by a Zeiss Axiovert 200 inverted epifluorescence microscope, coupled to a AxioCam MRc, and Axiovision software, Carl Zeiss Canada Ltd; original magnification $\times 20$) with quantitative estimates of the surface area covered by adherent platelets (middle) and captured platelet aggregate sizes (right). A, Platelet adhesion to recombinant von Willebrand factor ($n = 6$ mice/genotype). B, Platelet adhesion to murine fibrinogen, evaluating using $n = 8$ *Mmrn1*^{+/+} mice and $n = 6$ *Mmrn1*^{-/-} mice. Symbols indicate data for *Mmrn1*^{+/+} (solid bars and circles) and *Mmrn1*^{-/-} mice (open bars and circles)

whole blood, activated *Mmrn1*^{-/-} platelets showed a minor reduction in adhesion to Fg ($P = .03$), accompanied by a reduction in size of captured platelet aggregates ($P = .007$; Figure 4B), but normal adhesion to fibrin and Fn (Figure S8A-D in supporting information).

3.4 | MMRN1 binds to GPAGPOGPX motifs in fibrillar collagens, which enhance platelet adhesion and show high specificity for *Mmrn1*

Collagen Peptide Toolkits were used to determine the locations and sequences in fibrillar vessel wall collagens that bind MMRN1. rMMRN1 bound two Collagen Toolkit peptides, II-9 and III-38, that share a GPAGPOGPX sequence where X is valine (II-9) or glutamine (III-38; Figure 5A,B). Tests with truncated derivatives indicated that MMRN1 bound to GPAGPOGPX but not to other regions of III-38 (Figure 5C). In silico searches indicated that the GPAGPOGPX motif is unique to fibrillar collagens, and that the GPAGPOGPV locus (helix residues: 151--159) of peptide II-9 is poorly conserved in collagens I and III. Searches for motifs conserved with the MMRN1-binding sequence in peptide III-38 (GPAGPOGPQ, helix residues: 682--690), and searches for variants of GPAGPOGPX elsewhere in collagen I (which consists of one α_2 and two α_1 chains) identified GPAGPOGPI at helix residues 667 to 675 in D-period 3 of the $\alpha_1(I)$ triple helix, and GPAGSOGFQ in D-period 2 at residues 457 to 465 that aligns with a conserved GPAGPOGFQ sequence in $\alpha_2(I)$. GPAGPOGPI in collagen I overlaps in sequence alignments with GPAGPOGPQ in collagen III, which has a 9-residue extension at its N-terminus, offsetting helix numbering. Testing of these collagen I sequences as homotrimeric triple-helical peptides, in parallel with GPP (negative control) indicated that GPAGPOGPI ($P = .0002$), but not the variants GPAGPOGFQ ($P = .12$) or GPAGSOGFQ ($P = .52$), supported MMRN1 binding (Figure 5D).

As the GPAGPOGPX motifs that bind MMRN1 in human collagens I, II, and III are fully conserved in murine collagens, these motifs were further tested using peptide-coated wells and mouse platelets. In contrast to CRP-activated *Mmrn1*^{-/-} platelets (which showed minimal adhesion), CRP-activated *Mmrn1*^{+/+} platelets showed dose-dependent adhesion to GPAGPOGPQ and GPAGPOGPI (Figure 5E,F), indicating that GPAGPOGPX supports platelet adhesion by a *Mmrn1*-dependent mechanism.

Although CRP-activated human platelets did not significantly adhere to GPAGPOGPX peptides alone (Figure 6A), co-presentation of GFOGER with GPAGPOGPX peptides, or with the VWF-binding peptide III-23, enhanced platelet adhesion ($P \leq .006$; Figure 6B). When GFOGER was present, GPAGPOGPX peptides in combination with III-23 further enhanced platelet adhesion (Figure 6B,C). The enhancing effect of GPAGPOGPX on platelet adhesion to GFOGER was increased by CRP activation to induce MMRN1 release ($P \leq .007$, Figure 6D), either by adding CRP to the sample or to coating peptides ($P > .24$, Figure S9 in supporting information).

High shear flow experiments (1500 s^{-1}) with CRP-activated mouse platelets provided further evidence that GPAGPOGPX is

highly specific for *Mmrn1* as co-presentation of GFOGER with GPAGPOGPQ increased the size of captured aggregates formed by wild-type ($P < .0001$) but not *Mmrn1*^{-/-} ($P = .07$) platelets (Figure 7A,B). *Mmrn1*^{-/-} platelets were also noted to form smaller aggregates than wild-type platelets on surfaces coated with GFOGER and GPP only ($P < .001$, Figure 7A,B), suggesting that *Mmrn1* stabilizes platelet-platelet interactions through additional mechanisms.

4 | DISCUSSION

Our goal was to evaluate platelet function in *Mmrn1*-deficient mice and to identify motifs in collagen that support platelet adhesion by binding to MMRN1. Our main findings were: (a) partial and complete *Mmrn1* loss impairs platelet adhesion and thrombus formation in vivo without causing a severe bleeding phenotype; (b) MMRN1 binds to FG, fibrin, and FN, but is not essential for platelet adhesion to these proteins, or to rVwf; (c) *Mmrn1* loss preserves low shear and high shear platelet aggregation responses although it reduces platelet adhesion to fibrillar collagen and Fg, and the size of platelet aggregates captured onto these proteins; (d) partial and complete *Mmrn1* impairs static, low shear, and high shear platelet adhesion to collagen; (e) *Mmrn1* is not essential for platelet adhesion to rVwf or GFOGER but its loss reduces the size of platelet aggregates captured onto rVwf and GFOGER; and (f) fibrillar collagens that support platelet adhesion contain GPAGPOGPX motifs that are highly specific for *Mmrn1* and work synergistically with other motifs to promote platelet adhesion.

Many studies of knockout mice have used the FeCl₃-induced mesenteric vessel injury model to assess platelet adhesion and thrombus formation. $\alpha_2^{-/-}$,³⁵ *FcR γ* ^{-/-} (which do not express GPVI),³⁶ *Tsp1*^{-/-},³⁷ *pFn*^{-/-},^{38,39} *Fg*^{-/-},⁴⁰ and *Vn*^{-/-} mice⁴¹ show impairments in one or two parameters of platelet adhesion and thrombus formation evaluated by this model. With *Mmrn1*^{-/-} and *Mmrn1*^{+/-} mice, platelet adhesion and thrombus formation were similarly impaired from start to finish in FeCl₃-injured vessels, reflected by reduced initial and final platelet adhesion and some mice failing to form any substantial thrombus. *Mmrn1*^{-/-} and *Mmrn1*^{+/-} mice did not exhibit spontaneous or fatal bleeding or significant alterations in BT. These data indicate that partial and complete *Mmrn1* loss impairs platelet-rich thrombus formation without incurring major impairments to hemostasis. This contrasts with the severely prolonged BT, reduced survival, or spontaneous bleeding reported for *Vwf*^{-/-},⁴² *Fg*^{-/-},⁴³ $\beta_3^{-/-}$,⁴⁴ and *Gplba*^{-/-} mice⁴⁵—which also have impaired FeCl₃-induced thrombus formation. It is interesting that *Mmrn1*^{+/-} mice, which had a milder platelet *Mmrn1* deficiency than *Mmrn1*^{-/-} mice, had impaired high shear collagen adhesion, and impairments in platelet adhesion and thrombus formation in the FeCl₃ vessel injury model that were similar to, and not significantly different from, the impairments observed with *Mmrn1*^{-/-} mice. These observations suggest that *Mmrn1* haploinsufficiency reduces *Mmrn1* levels below what is needed to support *Mmrn1*-dependent aspects of platelet function.

While we found that *Mmrn1* is not required for platelet adhesion to Fg, fibrin, or Fn, its absence did reduce platelet adhesion, and the

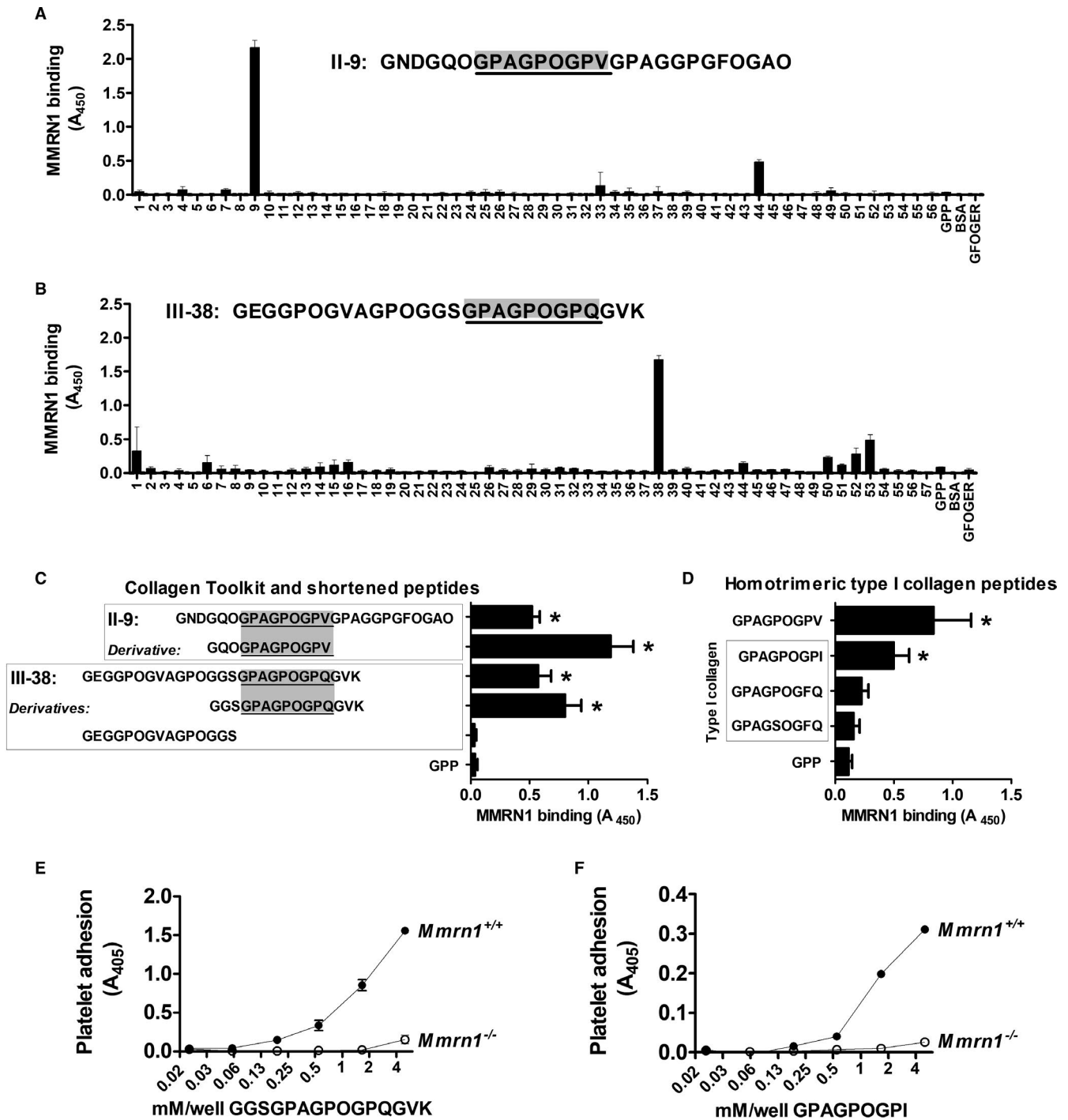


FIGURE 5 Multimerin 1 (MMRN1) binding to collagen, evaluated using Collagen Toolkit and other triple-helical peptides, and static platelet adhesion assays. Panels (A)–(B) show data from representative experiments to assess MMRN1 binding to Collagen Toolkit II (A) and Toolkit III (B) peptides, the control peptide GPP, and GFOGER. The sequence of the peptides showing the most binding is indicated in text. C, MMRN1 binding to Toolkit peptides II-9 and III-38 is compared to MMRN1 binding of shortened, derivatives of these peptides and GPP (negative control). D, MMRN1 binding to GPAGPOGPV and homotrimeric variants of the GPAGPOGPX sequence in collagen $\alpha 1(I)$ and $\alpha 2(I)$. E, Evaluation of the specificity of MMRN1-binding peptide GGSGPAGPOGPQGVK by static platelet adhesion assays using collagen-related peptide-activated $Mmrn1^{+/+}$ (average for $n = 4$ mice) or $Mmrn1^{-/-}$ (average for $n = 3$ mice) platelets. F, Similar static platelet adhesion assay evaluation of the MMRN1-specificity of GPAGPOGPI (average for $n = 3$ mice/group). In panels (A)–(C), absorbance values are corrected for non-specific binding to bovine serum albumin (BSA). Bars and whiskers in Panels (C) and (D) represent the average and standard deviation of three identical experiments, each performed in triplicate. Symbols in Panels (E) and (F), respectively, show data for $Mmrn1^{+/+}$ (solid) and $Mmrn1^{-/-}$ (open) mice, and absorbance values are corrected for non-specific adhesion by subtracting adhesion to GPP at each concentration tested.

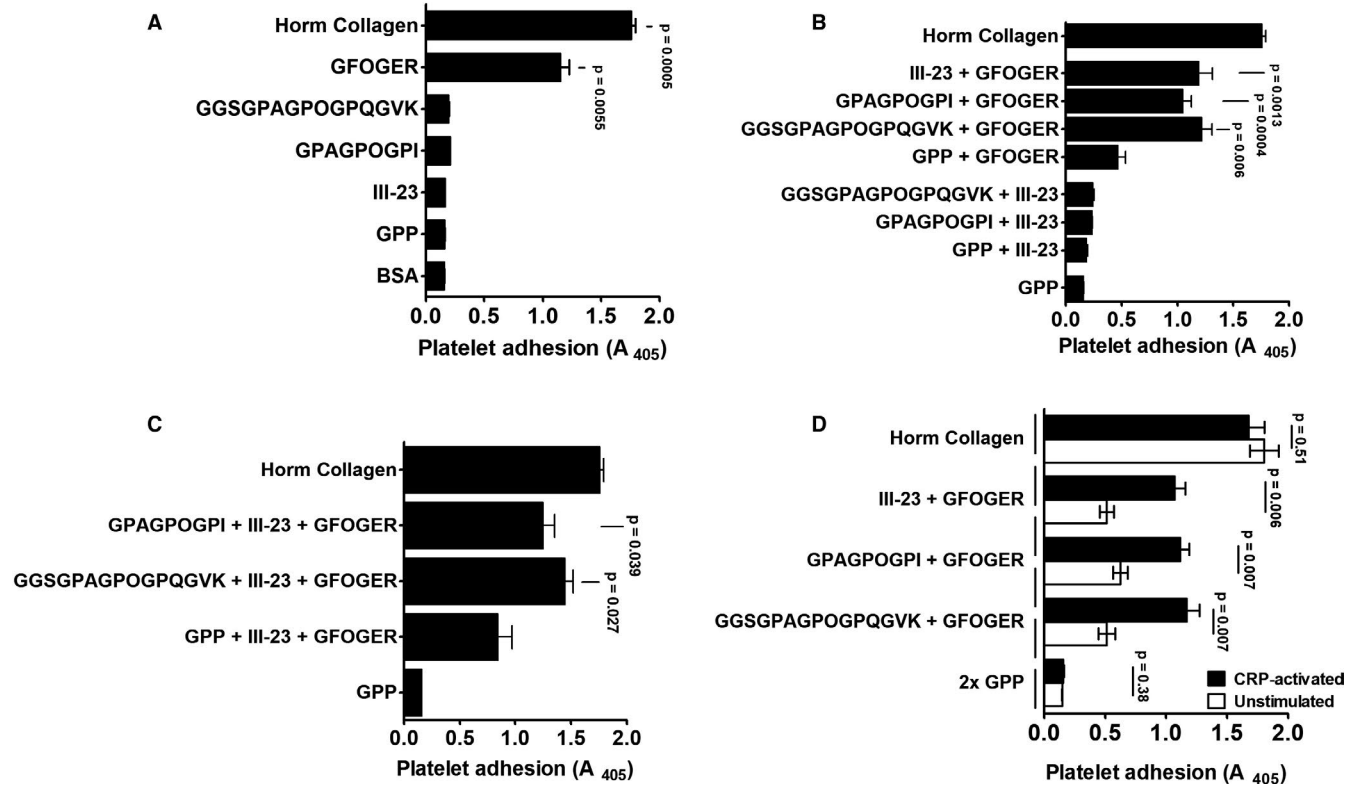


FIGURE 6 Synergistic effects of the multimerin 1 (MMRN1)-binding GPAGPOGPX peptides and other collagen mimetic peptides on human platelet adhesion. Panels show adhesion of human platelets pre-activated with 10 $\mu\text{g}/\text{mL}$ collagen-related peptide (CRP; to pre-expose platelet MMRN1 and von Willebrand factor [VWF] and activate platelet integrins), unless otherwise indicated. Data are shown as mean absorbance \pm standard error of the mean, for three different samples/group, each tested in triplicate to obtain a mean for each sample, evaluated with the indicated combination of peptides or with GPP (negative control) and Horm collagen (positive control). A, Platelet adhesion to all peptides except GFOGER was indistinguishable from background binding to GPP. B, The VWF-binding sequence III-23 and GPAGPOGPX peptides enhanced platelet adhesion to GFOGER but not to each other. C, Co-presentation of III-23 and GPAGPOGPX peptides increased platelet adhesion to GFOGER. D, Effect of platelet activation with 10 $\mu\text{g}/\text{mL}$ CRP on platelet adhesion to GFOGER and GFOGER co-presented with either GPAGPOGPX or III-23

size of platelet aggregates captured onto Fg- but not fibrin-coated surfaces under low shear flow. The latter discrepancies could reflect differences in the ultrastructure of surface-adsorbed Fg versus fibrin, and/or differences in Fg- and fibrin- $\alpha_{\text{IIb}}\beta_3$ binding interactions.^{46,47} It is also possible that the high-affinity conformation of $\alpha_{\text{IIb}}\beta_3$ or activation-induced receptor clustering is required for platelets to bind Mmrn1, as activation enhances human platelet adhesion to MMRN1.^{5,6} We suggest that Mmrn1 works synergistically with other proteins, including Fg and Vwf, to enhance platelet adhesion onto a growing platelet aggregate. The binding site(s) for MMRN1 on FG are unknown, but Mmrn1 does not appear to inhibit the ability of platelets to adhere to immobilized Fg, which occurs predominantly via the Fg γ -chain binding to $\alpha_{\text{IIb}}\beta_3$.⁴⁸ Further, we did not detect an influence of Mmrn1 on platelet adhesion to immobilized Fn. Blockade of $\alpha_{\text{IIb}}\beta_3$ partially inhibited static adhesion of *Mmrn1*^{-/-} and wild-type platelets to rMMRN1, similar to what we observed with human platelets,⁵ implicating the involvement of $\alpha_{\text{IIb}}\beta_3$ and other, yet-to-be-identified receptors in Mmrn1 binding.⁵

As platelets require activation for Mmrn1-mediated adhesion, we suggest that Mmrn1 promotes adhesion after release from activated platelets and/or endothelial cells. The ligation of VWF to GPIIb

induces activation of $\alpha_{\text{IIb}}\beta_3$ and Ca^{2+} mobilization in platelets, but it is insufficient for α -granule release,⁴⁹ which could explain why we saw similar adhesion of *Mmrn1*^{-/-} and *Mmrn1*^{+/+} platelets to rVwf. There was likely some non-intentional platelet activation in the experiments measuring platelet adhesion to rVwf at high shear given that *Mmrn1*^{-/-} platelets were captured into smaller aggregates. Nonetheless, our findings suggest that MMRN1 participates in platelet adhesion only after platelets are tethered and have secreted granule contents. As platelets adherent to collagen are activated, with granule content secretion, Mmrn1 could be more important for platelet adhesion to collagen than to Vwf, as our data suggest. Larger MMRN1 multimers preferentially stay bound to platelets,⁴ which might enhance the avidity of Mmrn1 interactions with collagen fibers and Vwf multimers. As both *Mmrn1*^{-/-} and *Mmrn1*^{+/-} platelets showed impaired platelet adhesion to collagen in high shear flow, mild quantitative (eg, 50%) reductions in Mmrn1 appear to be sufficient to impair platelet-collagen interactions, which could have clinical implications. Additionally, Mmrn1 could bridge $\alpha_{\text{IIb}}\beta_3$ -bound Fg on activated platelets to collagen, to further stabilize platelet adhesion. The idea that adhesive proteins bind one another to form large, macromolecular complexes has been proposed as a possible explanation for the supportive role of multimeric platelet VN,⁴¹

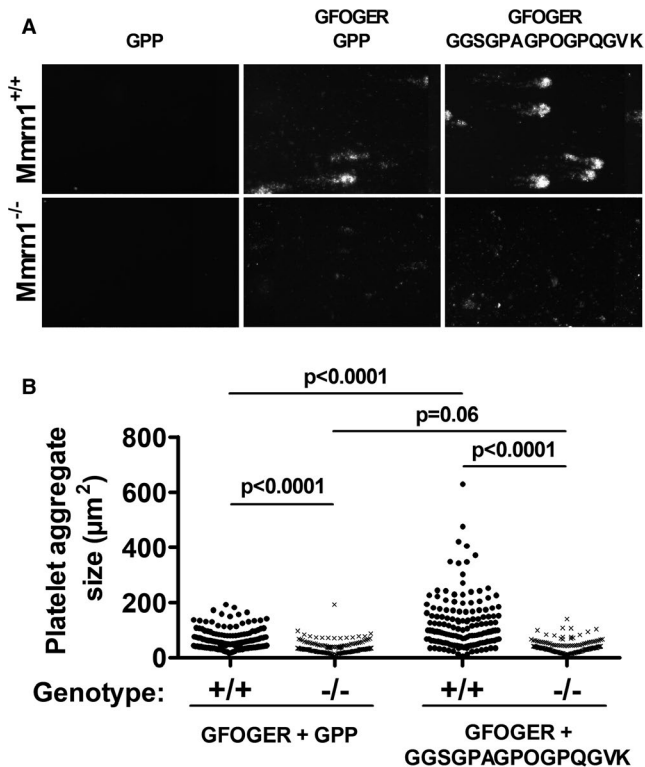


FIGURE 7 Adhesion of washed, collagen-related peptide (CRP)-activated wild-type and multimerin 1 (*Mmnr1*)-deficient mouse platelets to collagen peptides under high shear flow (1500 s^{-1}). A, Representative images show endpoint adhesion of DiOC6(3)-labeled CRP-activated *Mmnr1*^{+/+} and *Mmnr1*^{-/-} platelets to immobilized triple-helical collagen peptides, captured by a Zeiss Axiovert 200 inverted epifluorescence microscope coupled to a AxioCam MRC and Axiovision software (Carl Zeiss Canada Ltd.; original magnification $\times 20$), and (B) mean platelet aggregate size on triple-helical collagen peptides analyzed for each image captured ($n = 5$ mice/group, $n = 15$ images/experiment). Symbols in (B) represent *Mmnr1* genotype: +/+ (●) and -/- (x)

TSP-1,²¹ and insoluble (crosslinked) plasma FN in platelet aggregate formation,⁵⁰ and in platelet adhesion to collagen.⁵¹

Our observations that complete and partial *Mmnr1* loss impairs initial platelet adhesion and thrombus formation in the FeCl_3 vessel injury model suggests *Mmnr1* modifies macromolecular adhesive interactions in vivo. Potentially, *Mmnr1* might bind to shear-stretched Vwf multimers to form larger, heteropolymers that enhance platelet tethering and adhesion. As *Mmnr1* loss reduced the size of platelet aggregates that adhered to collagen, rVwf, Fg, and GFOGER peptides, we suggest that *Mmnr1* also functions to stabilize platelet–platelet interactions in wounds and injured vessels. Figure 8A summarizes the proposed role of *Mmnr1* in platelet adhesion.

The GPAGPOGPX motif that binds MMRN1 is unique to collagens and distinct from other motifs identified with Collagen Toolkits (Figure 8B),^{52–60} including those that bind VWF,³³ $\alpha_2\beta_1$,²⁹ and GPVI.⁶¹ While leukocyte-associated Ig-like receptor-1 (LAIR-1) binds to Collagen Toolkit peptide III-38, LAIR-1 binds to the repeated GPO

motifs in peptide III-38, not to the GPAGPOGPX sequence.⁵⁵ The conserved MMRN1-binding motif GPAGPOGPX lies at the same locus in the collagen $\alpha_1(\text{I})$ chain. The defective adhesion of *Mmnr1*-deficient platelets to GPAGPOGPX motifs that were evident in static, low shear, and high shear flow conditions suggests that *Mmnr1* supports platelet adhesion in wounds that expose blood to fibrillar collagen. Additionally, *Mmnr1*-GPAGPOGPX binding could be one of the VWF-independent mechanisms that mediates platelet adhesion and aggregate formation on collagen under low shear flow conditions.⁶²

The in vivo defects in platelet adhesion and platelet-rich thrombus formation of *Mmnr1*^{-/-} and *Mmnr1*^{+/-} mice may reflect other defects as collagen exposure in FeCl_3 injured vessels appears minimal,^{40,63} and the precise mechanisms that this model tests remain unclear.^{64,65} While $\alpha_2\beta_1$ and GpVI interact with fibrillar collagens to support platelet adhesion in vitro,^{32,61,66} impaired signalling, rather than impaired collagen interactions, is thought to underlie the impaired thrombus formation of α_2 ^{-/-} and *FcR γ* ^{-/-} (GpVI-deficient) mice in FeCl_3 injured vessels.^{35,36} *Mmnr1* loss could have other effects, given that MMRN1 binds factor V and can affect thrombin generation.⁶⁷ In our study, we assessed the consequences of complete and partial *Mmnr1* loss and in future studies, it would be interesting to test the contributions of platelet versus endothelial *Mmnr1* in adhesion and thrombus formation in vivo, as both cells store *Mmnr1* for activation-induced secretion, and studies of other adhesive proteins stored in these cells (eg, von Willebrand factor, fibronectin) have provided insights on the relative contributions of the platelet versus endothelial stores.

Collagens are ubiquitous proteins that represent ~30% of total protein mass in mammals,⁶⁸ with about 90% of collagens estimated to be type I fibrillar collagen.⁶⁹ Injuries that sever or rupture a vessel would expose blood to the collagen-rich outer layers of the vessel wall and extravascular connective tissues where *Mmnr1* binding to GPAGPOGPX motifs may be very relevant to platelet adhesion. Disease-causing mutations that impair MMRN1-collagen binding might affect platelet adhesion. While no pathogenic MMRN1 mutations are reported, G845R and G848R mutations in the GPAGPOGPX motif are associated with type II (perinatal lethal) osteogenesis imperfecta and a G852C mutation in GPAGPOGPQ is associated with type IV (vascular type) Ehlers-Danlos syndrome, which causes hematomas, hemothorax, and vessel rupture.^{70,71} Many mucocutaneous bleeding disorders remain uncharacterized and MMRN1 defects might go undetected by current bleeding disorder investigations. An assessment of platelet adhesion to collagen, and to combinations of CRP, GPAGPOGPX, and GFOGER peptides, could help identify cases of MMRN1 deficiency, but this would be a time- and resource-intensive undertaking. Nonetheless, platelet MMRN1 deficiency might account for some platelet function abnormalities noted in gray platelet syndrome, Quebec platelet disorder, and $\alpha\delta$ -storage pool deficiency.

In summary, our study provides direct evidence that *Mmnr1* contributes to platelet adhesion and thrombus formation in vivo, supports platelet adhesion and aggregate formation onto a variety of protein surfaces, and contributes to platelet adhesion to collagen through its interactions with *Mmnr1*-specific GPAGPOGPX motifs in vessel wall fibrillar collagens.

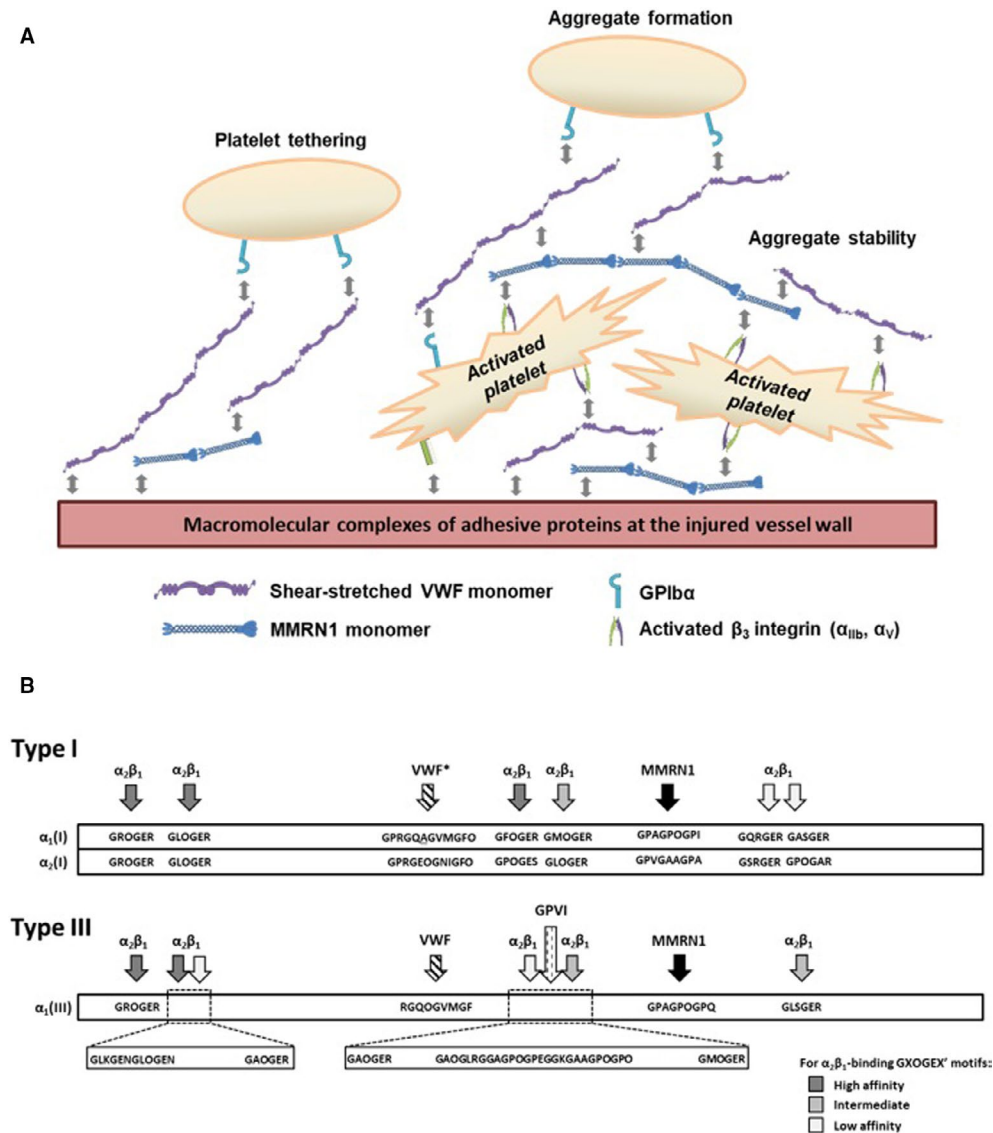


FIGURE 8 Proposed model of multimerin 1 (Mmrn1) functions in platelet adhesion and an updated model of the motifs in types I and III vessel wall fibrillar collagens that support platelet adhesion or activation. A, Proposed role of Mmrn1 in platelet adhesion. Following Mmrn1 release from platelets and endothelial cell storage granules, $\alpha_{IIb}\beta_3$, $\alpha_V\beta_3$, and other unidentified receptors mediate Mmrn1 binding to platelets. Mmrn1 binding to platelets increases the size and stability of platelet aggregates that are captured onto the macromolecular protein complexes that promote platelet-matrix and platelet-platelet interactions. Shear-exposed and matrix bound von Willebrand factor (Vwf), fibrin(ogen), and fibronectin in these macromolecular protein complexes provide multiple binding sites for Mmrn1 attachment. Additionally, at sites of injury that expose blood to fibrillar collagen, Mmrn1 binds to GPAGPOGXP motifs to synergistically increase platelet adhesion to collagen beyond the adhesion supported by Vwf- and $\alpha_2\beta_1$ -dependent mechanisms. B, Scale representation of the spatial arrangement of the functional sequences in the triple-helical (COL) domain of human type I (top) and type III (bottom) collagen that support platelet adhesion or activation. *The α_1 - α_1 - α_2 heterotrimer consisting of GPRGQAGVMGFO and GPRGEOGNIGFO in type I collagen has been verified to support VWF binding using heterotrimeric triple-helical peptides.⁷² GXOGER sequences that bind $\alpha_2\beta_1$, the VWF-binding sequence GPRGQOGVMGFO, and the GPVI-binding sequence GAOGLRGAGPOGPEGGKGAAGPOGPO have been previously described elsewhere [Colour figure can be viewed at wileyonlinelibrary.com]

ACKNOWLEDGMENTS

This work was supported by the Canadian Institutes of Health Research (CIHR) grant MOP 133474 (CPMH), Heart and Stroke Foundation of Ontario operating grants T6586 and NA 7214 (CPMH), CIHR grant MOP 119540 and CIHR Foundation Grant 389035 (HN), CIHR Foundation Grant FDN-154285 (DL), Wellcome Trust 094470/Z/10/Z (RWF), and the British Heart Foundation grant RG/15/4/31268 (RWF).

CONFLICTS OF INTEREST

RWF is Scientific Advisor and AB is the Lead Peptide Scientist at CambCol Laboratories Ltd. The other authors declare that they have no real or perceived conflicts of interest to disclose.

AUTHOR CONTRIBUTIONS

A. Leatherdale and D. Parker designed and conducted experiments, analyzed and interpreted the findings, and led the manuscript

writing, in collaboration with C. P. M. Hayward, who supervised the study. S. Tasneem designed and performed experiments with S. W. Hamaia and analyzed data. Y. Wang performed and analyzed the FeCl₃ vessel injury experiments. D. Bihan and A. Bonna designed and synthesized collagen mimetic peptides. D. Lillcrap provided recombinant mouse Vwf, contributed to experimental design and interpretation, and edited the manuscript. P. L. Gross provided essential tools, guidance on microscopy and experimental design, and edited the manuscript. H. Ni provided essential tools and led the experimental design and supervision of the FeCl₃ vessel injury experiments. B. W. Doble developed the strategy for generating Mmrn1-deficient mice, which was carried out by S. Tasneem. R. W. Farndale guided the studies using Collagen Toolkit peptides to map MMRN1 binding motifs, supervised collagen peptide synthesis, and interpretation of peptide binding data, and edited the manuscript.

ORCID

Peter L. Gross  <https://orcid.org/0000-0002-8698-7074>

Heyu Ni  <https://orcid.org/0000-0002-7621-2945>

Bradley W. Doble  <https://orcid.org/0000-0002-0260-2983>

Catherine P. M. Hayward  <https://orcid.org/0000-0002-2843-0817>

TWITTER

Catherine P. M. Hayward  @CatherineHayw15

REFERENCES

- Hayward CPM, Bainton DF, Smith JW, et al. Multimerin is found in the α -granules of resting platelets and is synthesized by a megakaryocytic cell line. *J Clin Invest.* 1993;91:2630-2639.
- Hayward CPM, Hassell JA, Denomme GA, Rachubinski RA, Brown C, Kelton JG. The cDNA sequence of human endothelial cell multimerin. *J Biol Chem.* 1995;270(31):18246-18251.
- Kika Veljkovic D, Cramer EM, Fichelson S, Massé J-M, Hayward CPM. Studies of α -granule proteins in cultured human megakaryocytes. *Thromb Haemost.* 2003;90:844-852.
- Hayward CPM, Smith JW, Horsewood P, Warkentin TE, Kelton JG. P-155, a multimeric platelet protein that is expressed on activated platelets. *J Biol Chem.* 1991;266:7114-7120.
- Adam F, Zheng S, Joshi N, et al. Analyses of cellular multimerin 1 receptors: in vitro evidence of binding mediated by α IIb β 3 and α V β 3. *Thromb Haemost.* 2005;94:1004-1011.
- Tasneem S, Adam F, Minullina I, et al. Platelet adhesion to multimerin 1 in vitro: influences of platelet membrane receptors, von Willebrand factor and shear. *J Thromb Haemost.* 2009;7:685-692.
- Parker DN, Tasneem S, Farndale RW, et al. The functions of the A1A2A3 domains in von Willebrand factor include multimerin 1 binding Cellular Haemostasis and Platelets. *Thromb Haemost.* 2016;116:87-95.
- Counts RB, Paskell SL, Elgee SK. Disulfide bonds and the quaternary structure of factor VIII/von Willebrand factor. *J Clin Invest.* 1978;62:702-709.
- Mosher DF. Organization of the provisional fibronectin matrix: control by products of blood coagulation. *Thromb Haemost.* 1995;74:529-533.
- Bae E, Sakai T, Mosher DF. Assembly of exogenous fibronectin by fibronectin-null cells is dependent on the adhesive substrate. *J Biol Chem.* 2004;279(34):35749-35759.
- Pickering JG, Chow LH, Li S, et al. α 5 β 1 integrin expression and luminal edge fibronectin matrix assembly by smooth muscle cells after arterial injury. *Am J Pathol* American Society for Investigative Pathology. 2000;156:453-465.
- Seiffert D, Schleeff RR. Two functionally distinct pools of vitronectin (VN) in the blood circulation: Identification of a heparin-binding competent population of VN within platelet α -granules. *Blood.* 1996;88:552-560.
- Stockman A, Hess S, Declerck P, Timpl R, Preissner KT. Multimeric vitronectin. Identification and characterization of conformation-dependent self-association of the adhesive protein. *J Biol Chem.* 1993;268:22874-22882.
- Greenberg CS, Miraglia CC, Rickles FR, Shuman MA. Cleavage of blood coagulation factor XIII and fibrinogen by thrombin during in vitro clotting. *J Clin Invest.* 1985;75:1463-1470.
- Parise LV, Philips DR. Fibronectin-binding properties of the purified platelet glycoprotein IIb-IIIa complex. *J Biol Chem.* 1986;261:14011-14017.
- Gardner JM, Hynes RO. Interaction of fibronectin with its receptor on platelets. *Cell.* 1985;42:439-448.
- Seiffert D, Smith JW. The cell adhesion domain in plasma vitronectin is cryptic. *J Biol Chem.* 1997;272:13705-13710.
- Weisel JW, Nagaswami C, Vilaire G, Bennett JS. Examination of the platelet membrane glycoprotein IIb-IIIa complex and its interaction with fibrinogen and other ligands by electron microscopy. *J Biol Chem.* 1992;267:16637-16643.
- Kloczewiak M, Timmons S, Lukas TJ, Hawiger J. Platelet receptor recognition site on human fibrinogen. Synthesis and structure-function relationship of peptides corresponding to the carboxy-terminal segment of the gamma chain. *Biochemistry.* 1984;23:1767-1774.
- Wang Y, Gallant RC, Ni H. Extracellular matrix proteins in the regulation of thrombus formation. *Curr Opin Hematol.* 2016;23:280-287.
- Bonnefoy A, Hantgan R, Legrand C, Frojmovic MM. A model of platelet aggregation involving multiple interactions of thrombospondin-1, fibrinogen, and GPIIb/IIIa receptor. *J Biol Chem.* 2001;276:5605-5612.
- Wang Y, Carrim N, Ni H. Fibronectin orchestrates thrombosis and hemostasis. *Oncotarget.* 2015;6:6-7.
- Reheman A, Tasneem S, Ni H, Hayward CPM. Mice with deleted multimerin 1 and α -synuclein genes have impaired platelet adhesion and impaired thrombus formation that is corrected by multimerin 1. *Thromb Res Elsevier B.V.* 2010;125:e177-e183.
- Vaezzadeh N, Ni R, Kim PY, Weitz JI, Gross PL. Comparison of the effect of coagulation and platelet function impairments on various mouse bleeding models. *Thromb Haemost.* 2014;112:412-418.
- Kahr WHA, Lo RW, Li L, et al. Abnormal megakaryocyte development and platelet function in Nbeal2^{-/-} mice. *Blood.* 2013;122:3349-3358.
- Hayward CPM, Rivard GE, Kane WH, et al. An autosomal dominant, qualitative platelet disorder associated with multimerin deficiency, abnormalities in platelet factor V, thrombospondin, von Willebrand factor, and fibrinogen and an epinephrine aggregation defect. *Blood.* 1996;87:4967-4978.
- Pruss CM, Golder M, Bryant A, et al. Pathologic mechanisms of type 1VWD mutations R1205H and Y1584C through in vitro and in vivo mouse models. *Blood.* 2011;117:4358-4366.
- Pruss CM, Golder M, Bryant A, Hegadorn C, Haberichter S, Lillcrap D. Use of a mouse model to elucidate the phenotypic effects of the von Willebrand factor cleavage mutants, Y1605A/M1606A and R1597W. *J Thromb Haemost.* 2012;10:940-950.
- Raynal N, Hamaia SW, Siljander PRM, et al. Use of synthetic peptides to locate novel integrin α 2 β 1-binding motifs in human collagen III. *J Biol Chem.* 2006;281:3821-3831.

30. Morton LF, Hargreaves PG, Farndale RW, Young RD, Barnes MJ. Integrin $\alpha 2\beta 1$ -independent activation of platelets by simple collagen-like peptides: collagen tertiary (triple-helical) and quaternary (polymeric) structures are sufficient alone for $\alpha 2\beta 1$ -independent platelet reactivity. *Biochem J*. 1995;306:337-344.
31. Asselin J, Knight CG, Farndale RW, Barnes MJ, Watson SP. Monomeric (glycine-proline-hydroxyproline)₁₀ repeat sequence is a partial agonist of the platelet collagen receptor glycoprotein VI. *Biochem J*. 1999;339:413-418.
32. Knight CG, Morton LF, Peachey AR, Tuckwell DS, Farndale RW, Barnes MJ. The collagen-binding α -domains of integrins $\alpha 1\beta 1$ and $\alpha 2\beta 1$ recognize the same specific amino acid sequence, GFOGER, in native (triple-helical) collagens. *J Biol Chem*. 2000;275:35-40.
33. Lisman T, Raynal N, Groeneveld D, et al. A single high-affinity binding site for von Willebrand factor in collagen III, identified using synthetic triple-helical peptides. *Blood*. 2006;108:3753-3756.
34. Onley DJ, Knight CG, Tuckwell DS, Barnes MJ, Farndale RW. Micromolar Ca²⁺ concentrations are essential for Mg²⁺-dependent binding of collagen by the integrin $\alpha 2\beta 1$ in human platelets. *J Biol Chem*. 2000;275:24560-24564.
35. Kuijpers MJE, Pozgajova M, Cosemans JMEM, et al. Role of murine integrin $\alpha 2\beta 1$ in thrombus stabilization and embolization: contribution of thromboxane A₂. *Thromb Haemost*. 2007;98:1072-1080.
36. Dubois C, Panicot-Dubois L, Merrill-Skoloff G, Furie B, Furie BC. Glycoprotein VI-dependent and -independent pathways of thrombus formation in vivo. *Blood*. 2006;107:3902-3906.
37. Prakash P, Kulkarni PP, Chauhan AK. Thrombospondin 1 requires von Willebrand factor to modulate arterial thrombosis in mice. *Blood*. 2015;125:399-406.
38. Ni H, Yuen PST, Papalia JM, et al. Plasma fibronectin promotes thrombus growth and stability in injured arterioles. *Proc Natl Acad Sci USA*. 2003;100:2415-2419.
39. Wang Y, Reheman A, Spring CM, et al. Plasma fibronectin supports hemostasis and regulates thrombosis. *J Clin Invest*. 2014;124:4281-4293.
40. Ni H, Denis CV, Subbarao S, et al. Persistence of platelet thrombus formation in arterioles of mice lacking both von Willebrand factor and fibrinogen. *J Clin Invest*. 2000;106:385-392.
41. Reheman A, Gross PL, Yang H, et al. Vitronectin stabilizes thrombi and vessel occlusion but plays a dual role in platelet aggregation. *J Thromb Haemost*. 2005;3:875-883.
42. Denis C, Methia N, Frenette PS, et al. A mouse model of severe von Willebrand disease: defects in hemostasis and thrombosis. *Proc Natl Acad Sci USA*. 1998;95:9524-9529.
43. Suh TT, Holmback K, Jensen NJ, et al. Resolution of spontaneous bleeding events but failure of pregnancy in fibrinogen-deficient mice. *Genes Dev*. 1995;9(16):2020-2033.
44. Hodivala-Dilke KM, McHugh KP, Tsakiris DA, et al. $\beta 3$ -integrin-deficient mice are a model for Glanzmann thrombasthenia showing placental defects and reduced survival. *J Clin Invest*. 1999;103:229-238.
45. Ware J, Russell S, Ruggeri ZM. Generation and rescue of a murine model of platelet dysfunction: the Bernard-Soulier syndrome. *Proc Natl Acad Sci USA*. 2000;97:2803-2808.
46. Sivaraman B, Latour RA. The relationship between platelet adhesion on surfaces and the structure versus the amount of adsorbed fibrinogen. *Biomaterials Elsevier Ltd*. 2010;31:832-839.
47. Weisel JW, Litvinov RI. Fibrin formation, structure and properties. *Subcell Biochem*. 2017;82:405-456.
48. Springer TA, Zhu J, Xiao T. Structural basis for distinctive recognition of fibrinogen γC peptide by the platelet integrin $\alpha IIb\beta 3$. *J Cell Biol*. 2008;182:791-800.
49. Nesbitt WS, Kulkarni S, Giuliano S, et al. Distinct glycoprotein Ib/V/IX and integrin $\alpha IIb\beta 3$ -dependent calcium signals cooperatively regulate platelet adhesion under flow. *J Biol Chem*. 2002;277:2965-2972.
50. Reheman A, Yang H, Zhu G, et al. Plasma fibronectin depletion enhances platelet aggregation and thrombus formation in mice lacking fibrinogen and von Willebrand factor. *Blood*. 2009;113:1809-1817.
51. Bastida E, Escolar G, Ordinas A, Sixma JJ. Fibronectin is required for platelet adhesion and for thrombus formation on subendothelium and collagen surfaces. *Blood*. 1987;70:1437-1442.
52. Konitsiotis AD, Raynal N, Bihan D, Hohenester E, Farndale RW, Leitinger B. Characterization of high affinity binding motifs for the discoidin domain receptor DDR2 in collagen. *J Biol Chem*. 2008;283:6861-6868.
53. Hamaia SW, Pugh N, Raynal N, et al. Mapping of potent and specific binding motifs, GLOGEN and GVOGEA, for integrin $\alpha 1\beta 1$ using collagen toolkits II and III. *J Biol Chem*. 2012;287:26019-26028.
54. Xu H, Raynal N, Stathopoulos S, Myllyharju J, Farndale RW, Leitinger B. Collagen binding specificity of the discoidin domain receptors: Binding sites on collagens II and III and molecular determinants for collagen IV recognition by DDR1. *Matrix Biol International Society of Matrix Biology*. 2011;30:16-26.
55. Lebbink RJ, Raynal N, de Ruiter T, Bihan D, Farndale RW, Meyaard L. Identification of multiple potent binding sites for human leukocyte associated Ig-like receptor LAIR on collagens II and III. *Matrix Biol Elsevier B.V. and International Society of Matrix Biology*. 2009;28:202-210.
56. Howes JM, Bihan D, Slatter DA, et al. The recognition of collagen and triple-helical toolkit peptides by MMP-13: Sequence specificity for binding and cleavage. *J Biol Chem*. 2014;289:24091-24101.
57. Barrow AD, Raynal N, Andersen TL, et al. OSCAR is a collagen receptor that costimulates osteoclastogenesis in DAP12-deficient humans and mice. *J Clin Invest*. 2011;121:3505-3516.
58. Vadon-Le Goff S, Kronenberg D, Bourhis JM, et al. Procollagen C-proteinase enhancer stimulates procollagen processing by binding to the C-propeptide region only. *J Biol Chem*. 2011;286:38932-38938.
59. Giudici C, Raynal N, Wiedemann H, et al. Mapping of SPARC/BM-40/osteonectin-binding sites on fibrillar collagens. *J Biol Chem*. 2008;283:19551-19560.
60. Kalamajski S, Bihan D, Bonna A, Rubin K, Farndale RW. Fibromodulin interacts with collagen cross-linking sites and activates lysyl oxidase. *J Biol Chem*. 2016;291:7951-7960.
61. Jarvis GE, Raynal N, Langford JP, et al. Identification of a major GpVI-binding locus in human type III collagen. *Blood*. 2008;111:4986-4996.
62. Pugh N, Simpson AMC, Smethurst PA, De Groot PG, Raynal N, Farndale RW. Synergism between platelet collagen receptors defined using receptor-specific collagen-mimetic peptide substrata in flowing blood. *Blood*. 2010;115:5069-5079.
63. Eckly A, Hechler B, Freund M, et al. Mechanisms underlying FeCl₃-induced arterial thrombosis. *J Thromb Haemost*. 2011;9:779-789.
64. Barr JD, Chauhan AK, Schaeffer GV, Hansen JK, Motto DG. Red blood cells mediate the onset of thrombosis in the ferric chloride murine model. *Blood*. 2013;121:3733-3741.
65. Ciciliano JC, Sakurai Y, Myers DR, et al. Resolving the multifaceted mechanisms of the ferric chloride thrombosis model using an interdisciplinary microfluidic approach. *Blood*. 2015;126:817-824.
66. Knight CG, Morton LF, Onley DJ, et al. Collagen-platelet interaction: Gly-Pro-Hyp is uniquely specific for platelet Gp VI and mediates platelet activation by collagen. *Cardiovasc Res*. 1999;41:450-457.
67. Jeimy SB, Fuller N, Tasneem S, et al. Multimerin 1 binds factor V and activated factor V with high affinity and inhibits thrombin generation. *Thromb Haemost*. 2008;100:1058-1067.
68. Ricard S. The collagen family. *Cold Spring Harb Perspect Biol*. 2011;3:1-19.

69. Di Lullo GA, Sweeney SM, Korkko J, Ala-Kokko L, San Antonio JD. Mapping the ligand-binding sites and disease-associated mutations on the most abundant protein in the human, type I collagen. *J Biol Chem*. 2002;277:4223-4231.
70. De Paepe A, Malfait F. The Ehlers-Danlos syndrome, a disorder with many faces. *Clin Genet*. 2012;82:1-11.
71. Bodian DL, Chan TF, Poon A, et al. Mutation and polymorphism spectrum in osteogenesis imperfecta type II: implications for genotype-phenotype relationships. *Hum Mol Genet*. 2009;18:463-471.
72. Jalan AA, Sammon D, Hartgerink JD, et al. Chain alignment of collagen I deciphered using computationally designed heterotrimers. *Nat Chem Biol*. 2020;16:423-429.

SUPPORTING INFORMATION

Additional supporting information may be found online in the Supporting Information section.

How to cite this article: Leatherdale A, Parker D, Tasneem S, et al. Multimerin 1 supports platelet function in vivo and binds to specific GPAGPOGPX motifs in fibrillar collagens that enhance platelet adhesion. *J Thromb Haemost*. 2021;19:547–561. <https://doi.org/10.1111/jth.15171>